



ESASGD 2016

GIS-IDEAS (2016)

Conference Title: International Conference on GeoInformatics for Spatial-Infrastructure Development in Earth & Allied Sciences (GIS-IDEAS)

Enhancing classification result on multispectral images based on fractions of endmember

Binh Nguyen^a, Nga Nguyen^b

^a Hanoi University of Science, email: binhntt@hus.edu.vn

^b Louisiana State University, Baton Rouge, LA 70803, US

Abstract

Current studies in land cover faced up with difficulties in the classification process due to mixing up in land cover. Majority of researches in increasing the accuracy of classification results focused in reducing directly spectral mixing of individual pixels. However, this study aims to calculate the endmember value of objects as well as the proportion of Soil-Water-Vegetation in each pixel as a basis to integrate the value of surrounding objects in pixels, which play an important role in increasing the classification accuracy. The case study area of this research was in Hanoi with several difficulties in urban management. Outputs from proposed algorithm was compared between the two satellite datasets of Landsat 8 and Sentinel-2 to examine the methodology uncertainty and provide recommendations for further application in many different multi-spectral datasets.

Keywords: Type your keywords here, separated by semicolons ;

1. Introduction

Image classification plays an important role in the optimal use of remotely sensed data in terms of multi-temporal and wide ground coverage enabling people to update information and implement researches in a prompt, effective, time and effort saving manner. In years, space-borne remote sensing and image classification techniques are restricted by either spatial resolution of the image or sampling interval in the field in comparing with pixel size. Especially, for satellite systems with low and moderate resolutions such as Landsat with pixel size is 30m.

In reality, there are one or more than one object in a pixel, if the size of the objects is smaller than the pixel size. Thus, supervised classification, especially for mixed land cover, will be severely influenced by the pixel contamination. Many solutions for reducing pixel contamination were proposed and developed in order to improve the accuracy of the image classification. So far, however, most of the studies were focused on direct calculation for the reduction of pixel contamination rather than evaluation of spectral values (in endmember) of objects as well as the proportion of soil-water-vegetation in each pixel which has strong impacts on the accuracy of the image classification. In order to deal with mentioned issues, authors proposed the supervised classification approach based on spatial association between the pixels which were determined by the proportion of soil-water-vegetation in each pixel. Optical moderate resolution data (Landsat 8 OLI and Sentinel 2) were

piloted.

2. Theoretical bases

2.1. Methodology

In multispectral image processing, the separation of objects in each pixel is the segmentation process with primary spectral values in the image pixel. These separate spectral values are called the actual spectral values from the mixture of different spectral values. Objects in the same pixel are the typical example for actual spectral value. There are different objects in one sole pixel such as water, paddy land, or bare land. Each object will be called as one endmember. The spectral value of each object will then be called as actual spectral value. Mixed pixels can be considered as points in the n -dimensional scatter plot, where n is the number of spectral bands. In the 2-dimensional space, if 2 endmembers are mixed up, then the mixed pixels will be located on the line, and the pure endmembers will be located at the extremes of the mixed line. If 3 endmembers are mixed up, then the mixed pixels will be located within a triangle, and the pure endmembers will be located at the vertices of the triangle.

Let $s(x, y)$ be a spectrum of values obtained at the sensor for a certain pixel with spatial coordinates (x, y) in a multispectral image. This spectrum can be considered as a n -dimensional (n -D) vector (where n is the number of spectral bands) and may be modeled in terms of a linear combination of several endmember vectors e_i , $i=1, \dots, E$ according to the equations and constraints [1].

$$s(x, y) = \sum_{i=1}^E c_i e_i \quad (1)$$

$$\sum_{i=1}^E c_i = 1 \quad 0 \leq c_i \leq 1 \quad (2)$$

Where E is the number of endmembers needed to accurately model the original spectrum, and c_i is a scalar value representing the fractional coverage of endmember vector e_i in pixel (x, y) . The ideal case is that the coefficients in the linear combination are nonnegative and sum to 1, being, therefore, interpretable as cover fractions or abundances [2].

PVI (Perpendicular Vegetation Index) was a vegetation index proposed by Richardson and Wiegand. In PVI estimation, the soil line plays a crucial role. PVI is represented in the 2-dimensional coordinate system where the near infrared band aligns along the vertical axis (y) and red band aligns along the horizontal axis (x). In this coordinate system, the scatter plot of the study area is represented to support the differentiation of wet soil and bare land. The reflectance characteristics in the red and near infrared bands of soil-water-vegetation are described as: Endmember E_v (vegetation) is on the left of the soil line. Endmember E_s (soil) is the furthestmost point of the red band. Endmember E_w (water) is the closest point of the near infrared band.

Hence, in the 2-dimensional space made by the red and near infrared bands with soil-water-vegetation are the 3 endmembers, spectral triangle will be generated where vegetation is at the upper vertex, water in at the bottom left vertex and soil is at the remainder. Based on the relation between spatial locations of the pixels with endmembers, the proportion of soil-water-vegetation was estimated for each pixel.

2.2. Proposed methods

An arbitrary observation point $P(x_p, y_p)$ is assumed to be within the spectral triangle generated by the

03 vertices of soil-water-vegetation. Perpendicular lines was drawn from P to the edges of the triangle (fig. 1). The lengths of lines PV, PS, PW represent for proportion of each factor in a pixel, PW represent for proportion of each factor in a pixel.

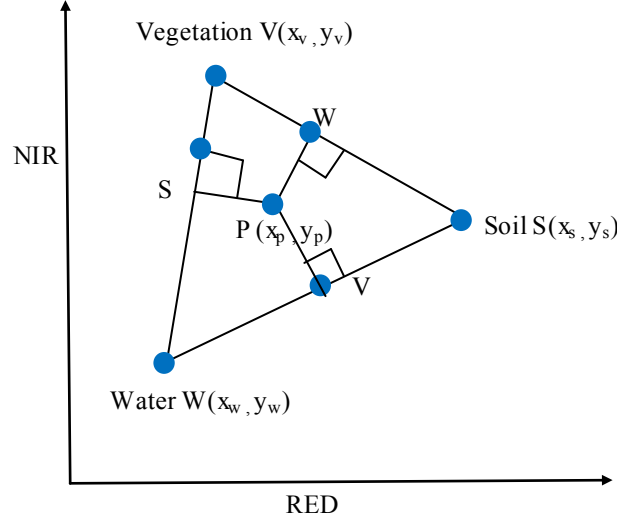


Fig. 1. Estimation of soil-water-vegetation proportion in a pixel [6]

With each observation point $P(x_p, y_p)$, soil-water-vegetation proportion can be estimated using following steps:

Step 1: To calculate the maximum and minimum in the red and near infrared bands for later calculation of $V(x, y_v = y_{\max})$; $W(x_w = x_{\min}, y_w = y_{\min})$; $S(x_s = x_{\max}, y_s)$

Step 2: To restrict calculation within the spectral triangle:

$$a_{ws} * RED + b_{ws} NIR + c_{ws} = 0 \quad (3)$$

$$a_{vs} * RED + b_{vs} NIR + c_{vs} = 0 \quad (4)$$

$$a_{vw} * RED + b_{vw} NIR + c_{vw} = 0 \quad (5)$$

Step 3: To calculate the 9 parameters ($a_{ws}, b_{ws}, c_{ws}, a_{vs}, b_{vs}, c_{vs}, a_{vw}, b_{vw}, c_{vw}$)

To calculate a_{ws}, b_{ws}, c_{ws} for line $a_{ws}x + b_{ws}y + c_{ws} = 0$ (WS):

$$a_{ws} = y_w - y_s \quad (6)$$

$$b_{ws} = x_s - x_w \quad (7)$$

$$c_{ws} = x_w(y_s - y_w) + y_w(x_w - x_s) \quad (8)$$

Similarly to equations (1, 2 and 3) to calculate $a_{vs}, b_{vs}, c_{vs}, a_{vw}, b_{vw}, c_{vw}$

Step 4: To calculate the lengths of PV, PS, PW

$$PV = \frac{|a_{ws} * x_v + b_{ws} y_v + c_{ws}|}{\sqrt{(a_{ws}^2 + b_{ws}^2)}} \quad (9)$$

Similarly to calculate the lengths of PW, PS.

Matlab programming language, a digital calculating environment and the fourth generation programming language by MathWorks, was used for processing and calculation. MatLab can be used to solve technically computing issues, especially image processing, faster and easier-to-understand than traditional programming languages. The two datasets captured in 2015 Landsat 8 and Sentinel 2, covering Hanoi city, where many difficulties in urban management located due to the mixing up in land cover, were used for experiment. The Landsat 8 (path 127 and row 45) image has less than 10% cloud cover while the Sentinel 2 (segment 48QWJ) image has a cloud cover of 24.09%. Both were downloaded online and pre-processed products. A cloud cover mask was used to remove effect of cloud on classification results.

3. Results and discussion

3.1. Endmember classification for Landsat 8 dataset

The first experiment was run on the Landsat 8 OLI acquired on June 01st 2016 (30x30 m resolution) covering the Hanoi area. In a pixel, the soil-water-vegetation proportion shall determine a certain pixel to belong to a specific class (or layer). However, observation and comparison can be made between proposed method and another supervised classification technique (Maximum Likelihood), where pixels containing soil are classified

into two classes as wet and dry based on the percentage of water in that specific pixel. Outputs of the two methods are represented in figure below.

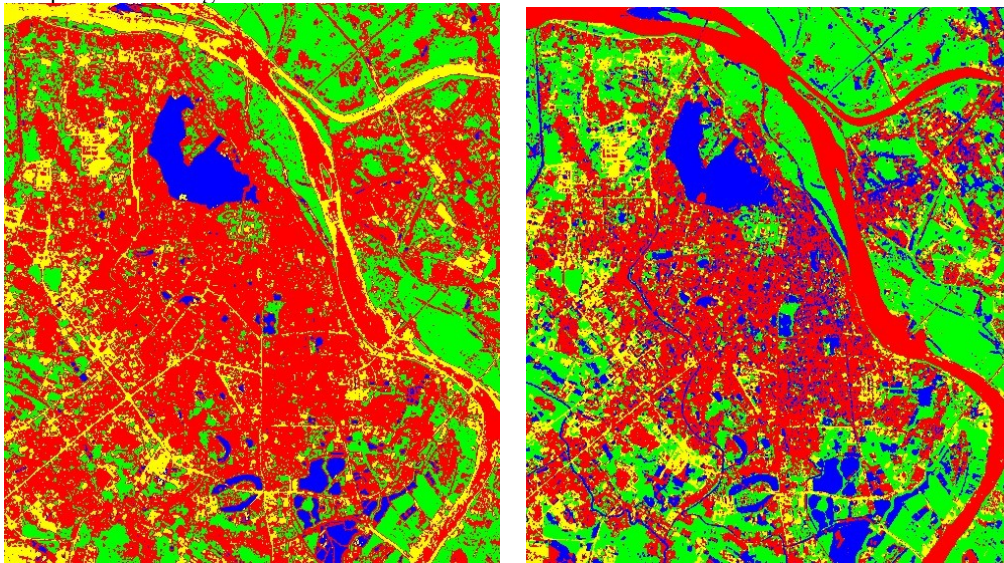


Fig. 4. (a) Image classified by Maximum Likelihood; (b) Image classified by the proposed method.

Table 1. Quantity of pixels and area of objects in the two different classified images

No	Object	Quantity of pixels			Area			Remark
		Maximum Likelihood	Proposed method	Variation	Maximum Likelihood	Proposed method	Variation	
1	Vegetation	66746	92700	25954	60071400	83430000	23358600	
2	Water	12135	41065	28930	10921500	36958500	26037000	
3	Wet soil	156147	111339	44808	140532300	10020510	40327200	
4	Dry soil	39508	29432	10076	35557200	26488800	9068400	

Table 2. Accuracy of classification result for Landsat 8 imagery

No	Compared characteristics	Raw Image	Maximum Likelihood	Proposed method
1	Linear hydrology			
2	Static water			
3	Linear transportation			

Linear objects such as river were classified well using the proposed method due to the restrictions of errors from sampling (training data) as well as pixel contamination. In specific, the Red river area was classified as soil due to the enormous amount of alluvium, which can be seen as in accordance with the proposed method (table 1 and 2).

3.2. Endmember classification for Sentinel-2 dataset

The imagery from Sentinel-2 satellite acquired on June 18th 2016 (10m resolution) covering Hanoi area was used for this experiment. Despite the spatial resolution of Sentinel-2 is higher than Landsat 8, cloud cover in Sentinel-2 remains high (above 24.09%). Band 10 of Sentinel-2 was used to eliminate large cloud cover from the estimation.

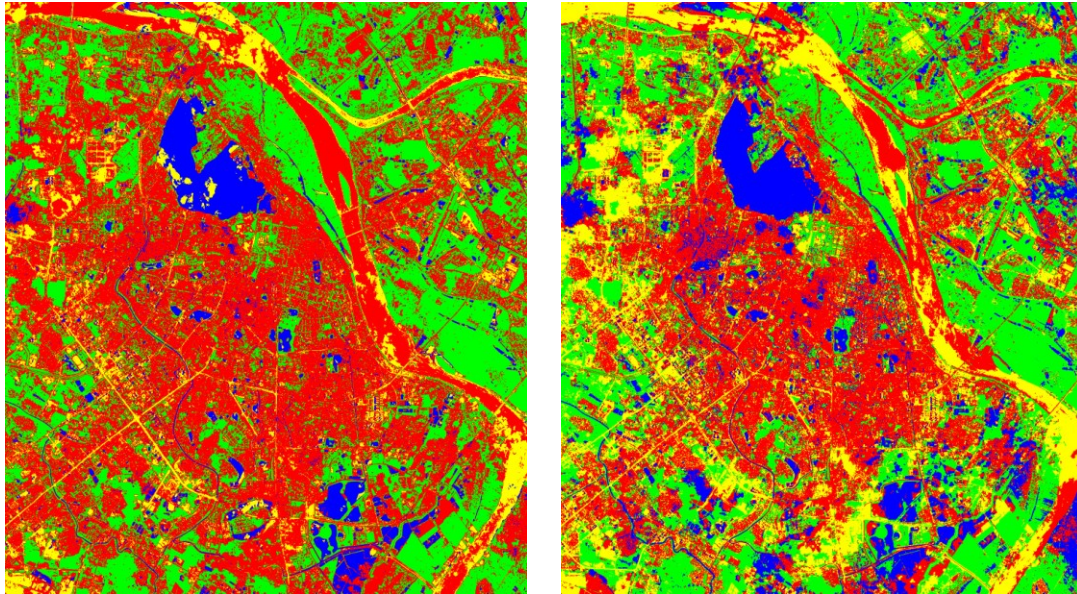


Fig. 5. (a) Image classified by Maximum Likelihood; (b) Image classified by the proposed method.

Table 3. Quantity of pixels and area of objects in the two different classified images

No	Object	Quantity of pixels			Area			Remark
		Maximum Likelihood	Proposed method	Variation	Maximum Likelihood	Proposed method	Variation	
1	Vegetation	807048	782166	24882	80704800	7821660	72883140	
2	Water	157053	269502	112449	15705300	2695020	13010280	
3	Wet soil	105385	941286	835901	10538500	9412860	112564	
4	Dry soil	1396516	473048	923468	139651600	4730480	134921120	


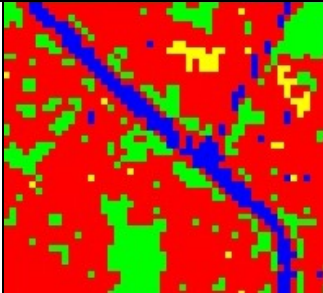



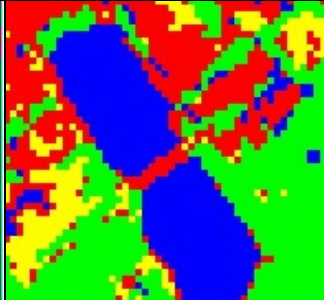



The two image classification techniques are influenced by cloud cover, but the proposed method showed higher accuracy in image classification, especially for linear objects (table 3 and 4).

3.3. Proposed methods uncertainty

Classification outputs of the two satellite datasets from proposed algorithm were compared to examine the methodology uncertainty and provide recommendations for further application in many different multi-spectral datasets.

As can be seen from the endmember classification, the proposed method showed dominant advantages in the results for Landsat 8 than Sentinel -2. This could be explained as the nature of classified data in which Landsat 8 image has lower resolution (30x10 m) in comparison to Sentinel -2 (10x10 m). The lower resolution causes more noises in mixed area and will reduce the accuracy if using Maximum Likelihood classification approach. Proposed method is more effective in classifying this low resolution data because its algorithm will remove all noise effect. This shows a promising application of this approach in enhance the accuracy for land cover mapping using free data as Landsat 8 in future.

Table 4. Accuracy of classification result for Sentinel-2 imagery

No	Compared characteristics	Raw Image	Maximum Likelihood	Proposed method
1	Linear hydrology			
2	Static water			
3	Linear transportation			

4. Conclusion

The proposed method to calculate the endmember value of objects as well as the proportion of Soil-Water-Vegetation in each pixel as a basis to integrate the value of surrounding objects in pixels, showed a simple, fast and effective approach to increase the classification accuracy. The proposed algorithm was applied in a case study in Hanoi which face difficulties in land-use mapping because of complicated land cover. The result from applying this approach to process the two satellite datasets of Landsat 8 and Sentinel-2 to enhance the land cover classification in Hanoi, a complicated location for land cover mapping because of mixed-up object, examine the methodology uncertainty and provide recommendations for further application in many different multi-spectral datasets. If widely apply, it will bring higher accuracy to urban land cover mapping, compared to traditional methods.

REFERENCES

- [1] Antonio Plaza, Pablo Martínez, Rosa Pérez, and Javier Plaza, 2002, "Spatial/Spectral Endmember Extraction by Multidimensional Morphological Operations"
- [2] C. A. Bateson, G. P. Asner, and C. A. Wessman, 2000, "Endmember bundles: A new approach to incorporating endmember variability into spectral mixture analysis," *IEEE Trans. Geosci. Remote Sensing*, vol. 38, pp.1083–1094
- [3] M. Petrou and P. G. Foschi, 1999, "Confidence in linear spectral unmixing of single pixels," *IEEE Trans. Geosci. Remote Sensing*, vol. 37, pp.624–626.
- [4] F. A. Kruse, 1998, "Spectral identification of image endmembers determined from AVIRIS data," in *Summaries of the VII JPL Airborne Earth Science Workshop*, Pasadena, CA
- [5] J. W. Boardman, F. A. Kruse, and R. O. Green, 1995, "Mapping target signatures via partial unmixing of AVIRIS data," in *Summaries of the V JPL Airborne Earth Science Workshop*, Pasadena, CA
- [6] Pham Minh Hai, 2015. *Studying a technical method to increase land cover classification accuracy*, Institutional Project, Vietnam institute of Geodesy and Cartography